Feeding Biochar to Cows: An Innovative Solution for Improving Soil Fertility and Farm Productivity

20 authors, including:

S. D. Joseph
UNSW Sydney
103 PUBLICATIONS   **6,930** CITATIONS

Kathy Dawson
Government of Western Australia
1 PUBLICATION   **12** CITATIONS

David Richard Graham Mitchell
University of Wollongong
163 PUBLICATIONS   **2,553** CITATIONS

Aditya Rawal
UNSW Sydney
60 PUBLICATIONS   **825** CITATIONS

Some of the authors of this publication are also working on these related projects:

Project Ilya Taranuk's Ph.D. work View project

Project Vitamin NMR View project

Feeding Biochar to Cows: An Innovative Solution for Improving Soil Fertility and Farm Productivity

Stephen JOSEPH[1,2,3,10,*], Doug POW[4], Kathy DAWSON[5], David R. G. MITCHELL[3], Aditya RAWAL[9], James HOOK[9], Sarasadat TAHERYMOOSAVI[2], Lukas VAN ZWIETEN[6], Joshua RUST[6], Scott DONNE[1], Paul MUNROE[3], Ben PACE[2], Ellen GRABER[8], Torsten THOMAS[7], Shaun NIELSEN[7], Jun YE[7], Yun LIN[1], Genxing PAN[10], Liqiang LI[10] and Zakaria M. SOLAIMAN[11]

[1] *Discipline of Chemistry, University of Newcastle, Callaghan 2308 (Australia)*
[2] *School of Materials Science and Engineering, University of New South Wales, Sydney 2052 (Australia)*
[3] *Electron Microscopy Center, AIIM, University of Wollongong, Wollongong 2522 (Australia)*
[4] *MarronBrook Farm, Manjimup 6258 (Australia)*
[5] *Warren Catchments Council, 52 Bath St, Manjimup 6258 (Australia)*
[6] *Wollongbar Primary Industries Institute, NSW Department of Primary Industries,1243 Bruxner Highway, Wollongbar 2477 (Australia)*
[7] *Centre for Marine Bio-Innovation, School of Biotechnology and Biomolecular Sciences, The University of New South Wales, Sydney (Australia)*
[8] *Institute of Soil, Water and Environmental Sciences, The Volcani Center, Agricultural Research Organization, POB 6, Bet Dagan 50250 (Israel)*
[9] *Mark Wainwright Analytical Centre, University of New South Wales, Kensington 2052 (Australia)*
[10] *Institute of Resources, Ecosystem and Environment of Agriculture, Nanjing Agricultural University, Nanjing 210095 (China)*
[11] *Soil Biology and Molecular Ecology Group, School of Earth and Environment (M087), The University of Western Australia, Crawley 6009 (Australia)*

ABSTRACT

Addition of biochar produced through thermal decomposition of biomass has been seen as a strategy to improve soils and to sequester carbon (C), but wide scale implementation of the technology requires to devise innovative profitable solutions. To develop biochar utilisation with an integrated system approach, an innovative program was implemented in 2012 on a 53-ha farm in Western Australia to determine the costs and benefits of integrating biochar with animal husbandry and improvement of pastures. Biochar was mixed with molasses and fed directly to cows. The dung-biochar mixture was incorporated into the soil profile by dung beetles. We studied the changes in soil properties over 3 years. Biochar extracted from fresh dung and from the soil to a depth of 40 cm was characterised. A preliminary financial analysis of the costs and benefits of this integrated approach was also undertaken. The preliminary investigation results suggested that this strategy was effective in improving soil properties and increasing returns to the farmer. It was also concluded that the biochar adsorbed nutrients from the cow's gut and from the dung. Dung beetles could transport this nutrient-rich biochar into the soil profile. There was little evidence that the recalcitrant component of the biochar was reduced through reactions inside the gut or on/in the soil. Further research is required to quantify the long-term impact of integrating biochar and dung beetles into the rearing of cows.

Key Words: animal husbandry, biochar, C sequestration, dung beetles, financial benefit, pasture

INTRODUCTION

Activated carbon (C), and more recently biochar, have been used as a supplement in animal feed. McHenry (2010) and Blackwell *et al.* (2009) both devised the case for integrating biochar into production of meat, both as a feed additive, as a low cost method of applying biochar to soils and as a potential bedding material. McHenry (2010) saw feeding biochar as a method of reducing inputs of chemical fertilisers, improving soil properties and C sequestration. Previous research has also identified biochar as a potential product which can improve animal health (Van *et al.*, 2006; Gerlach *et al.*, 2014). Calvelo Pereira *et al.* (2014) found

---

*Corresponding author. E-mail: joey.stephen@gmail.com.

that biochar mixed with silage or hay did not have a negative effect on rumen chemistry during *in vitro* incubations. Biochar can also assist in reducing the risk of bioaccumulation of organic pollutants, such as dichlorodiphenyltrichloroethane (DDT) and Dieldrin (Hale *et al.*, 2011)

The Western Australian beef herd consists of approximately two million head of cattle, half of which are free range on extensive pastoral stations in the northern rangelands, while the remainders graze the pastures of the agricultural region of the south and south-west of the state. In 2011/2012 the Australian Bureau of Statistics estimated that the gross value of beef production in Western Australia was \$517 million. The state exported 220 000 live cattle, valued at \$154 million, in addition to 99 000 t of boxed beef products worth \$68 million in 2012. Mature animals produce about 18 kg of wet dung each day, giving a total production of over 36 000 000 t dropped onto Western Australian pastures each year. In some areas the effluent from this dung has flowed into the river systems causing eutrophication (Doube *et al.*, 2003). Dung beetles (*Bubas bison*) are considered to have the potential to transform this pollutant into a multi-million dollar production benefit (Fincher, 1981), to increase the permeability of soil to water (Doube *et al.*, 2003), and to significantly reduce the pollution of water bodies.

Surface dung contributes to reliance on veterinary chemicals to control resultant parasite populations which dung harbors. The loss of nitrogen (N) from dung due to volatilization contributes to the need for higher applications of fertilisers, with the subsequent effect of increasing soil acidity (Haynes and Naidu, 1998). A major problem is the increase in acidity of the soil and the need to increase the amount of su-

perphosphate added to the pastures, as well as a need to supplement feed with expensive hay. The cost of the conventional practice (CP) of supplementary feeding grass-fed cattle with hay and silage throughout the annual pasture non-growing period has increased due to recent severe droughts (Dairy Australia, 2015).

An innovative program has been implemented on a 53-ha farm in Western Australia (Brook Farm 58°34.18′ S, 116°8.34′ E) in 2012 to determine the costs and benefits of using biochar as a feed supplement and dung beetles as a means of incorporation of both the dung and biochar into the soil profile. Dung beetles had been introduced by an adjoining property in 1990 and these beetles had migrated to the farm by 2009 when the present owner purchased it. Until 2009, extensive horticulture combined with grazing had been undertaken. Farming practice included the use of superphosphate, and historically, the organochlorine insecticides DDT, dichlorodiphenyldichloroethylene (DDE) and Dieldrin were applied. In 2009, the present owner converted the farm for the raising of steers and no further insecticides or herbicides were used.

In this program biochar was provided as a feed supplement to 60 cows. Dung beetles incorporated the biochar and dung into the pastures to a depth of approximately 40 cm (Fig. 1). This paper reports a preliminary study to determine the changes that had taken place in the field that had biochar addition *via* animal feed application, over a 3-year period, to examine the characteristics of the biochar after digestion through the animal and after soil incorporation by dung beetles, and to summarise the changes in the cost of production that had been reported by the farmer. A detailed study of the changes in all the fields, along
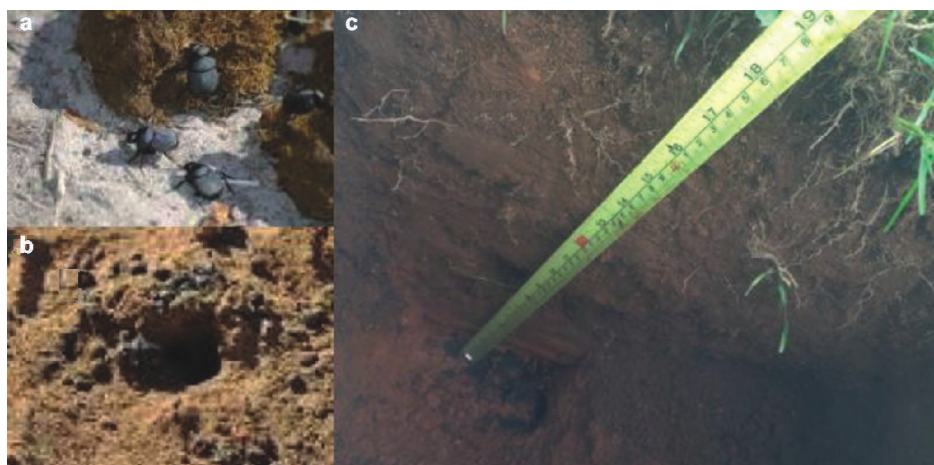

Fig. 1 (a) Dung beetles processing dung with biochar; (b) dung beetles pack dung-biochar mixture into tunnels dug deep into the soil profile; (c) biochar at bottom of trench where samples were taken.

with the economic benefits, will be reported in a subsequent work.

MATERIALS AND METHODS

Method of feeding cows and dung beetle application

In 2012 a new animal husbandry practice was introduced. Cows were fed with a mixture of 0.1 kg day^{-1} of molasses with 0.33 kg day^{-1} of jarrah wood biochar (known as Simcoa biochar) which was purchased from Simcoa Pty Ltd. (Kemerton, Australia). Biochar was first fed to cows in the winter to coincide with the active season of the dung beetle (mid-April emergence until mid-October). In 2012–2014 biochar was fed to cows on all 4 pasture paddocks of the farm at the same period of the year.

Soil and biochar samples

The soil in the field (known as "East field"), where biochar was first added in 2012, was classed as a Chromosol (Department of Agriculture and Food Western Australia). In 2011, before the introduction of the biochar, 30 core soil samples were taken from a transect across the "East field" to a depth of 10 cm. These were combined, put through a 2-mm sieve, riffled and analysed by CSPB Pty Ltd. (Perth, Australia). Cows were fed with biochar from 2012 in this field and dung beetles incorporated the resulting dung into the soil profile (Fig. 1). Soil sampling was carried out along the same transect in 2015 and a similar analysis to that carried out in 2011 was undertaken. The results are summarised in Table I. Biochar from part of the bulked soil sample was extracted using the technique reported by Joseph *et al.* (2010). Sufficient biochar was collected to determine the C, N, Colwell P, pH (CaCl$_2$), electrical conductivity (EC) and elemental composition of the aged biochar.

Characterisation of the biochar following digestion by the cow and after incorporation into the soil, involved a sampling procedure similar to that used by Downie *et al.* (2011). Six soil samples were taken along this transect to a depth of 40 cm in the "East field" where animals had grazed for 3 years and where dung beetle tunnels were visible. A core sampler was used to take samples at 0–5 cm. A trench was dug to 20–30 cm and then to 30–40 cm where a spatula was used to collect soil around the dung-filled tunnels at each depth (Fig. 1). All soil samples were amalgamated and sent to New South Wales (NSW) Department of Primary Industries' Wollongbar Environmental Laboratory for analysis of EC, pH, total N, organic C, P, K, available N as NH$_4^+$ and NO$_3^-$, Colwell P, metals and exchangea-

TABLE I

Some basic properties of soil in the study field in 2011 (before the introduction of biochar) and 2015 (biochar addition *via* animal feed application over a 3-year period)

Property	2011	2015
Electrical conductivity (dS m^{-1})	0.063	0.124
pH (H$_2$O)	5.9	5.9
pH (CaCl$_2$)	4.9	5.2
Total N (g kg^{-1})	NM[a)]	4.7
Total C (g kg^{-1})	NM	58.1
Total P (mg kg^{-1})	NM	938
Colwell P (mg kg^{-1})	49	102
Colwell K (mg kg^{-1})	55	205
KCl-extractable NH$_4^+$-N (mg kg^{-1})	21	10
KCl-extractable NO$_3^-$-N (mg kg^{-1})	15	33
Total organic C (g kg^{-1})	41.7	46.7
Al (cmol(+) kg^{-1})	< 0.100	0.168
Ca (cmol(+) kg^{-1})	5.10	6.78
K (cmol(+) kg^{-1})	0.17	0.50
Mg (cmol(+) kg^{-1})	0.63	0.76
Na (cmol(+) kg^{-1})	0.10	0.18

[a)]Not measured.

ble cations as per the procedures given in Van Zwieten *et al.* (2010). Biochar was separated and washed from the amalgamated soil samples at each depth using the procedures described by Lin *et al.* (2012b). The separated biochar was labeled as D1, D2 and D3 for the depths of 0–5, 20–30 and 30–40, respectively. Freshly deposited dung was also collected and stored at approximately 4 °C until the biochar could be separated out using the soil extraction method described by Lin *et al.* (2012b). This biochar extracted from the dung was labeled as D0.

Fresh and aged biochars

Jarrah wood biochar was produced in a vertical retort with a residence time of 12 h at a maximum temperature of 600 °C. Some properties of the biochar have been published by Dempster *et al.* (2012). Further analysis has been carried out as part of this work. The ultimate, proximate and ash analysis were completed by Bureau Veritas Pty Ltd. (Singleton, Australia). Detailed examination of the fresh biochar was also reported by Lin *et al.* (2012a). To complement this work labile organic species were extracted from the jarrah wood biochar and analysed using gas chromatography-mass spectrometry (GC-MS) (Chia *et al.* 2014).

Scanning electron microscopy (SEM) analysis of the microstructure of incorporated biochars was performed using a ZEISS Sigma SEM (Munich, Germany) fitted with a Bruker energy dispersive X-ray spectrometer (EDS) (Bruker Corporation, Berlin, Germany). To provide detailed microstructural, crystallographic

and micro-chemical analysis, both transmission electron microscopy (TEM) and scanning transmission electron microscopy (STEM) were undertaken using a JEOL ARM200F aberration corrected STEM (JEOL, Tokyo, Japan) fitted with an electron energy loss spectrometer (EELS) and a JEOL large area EDS detector. To help determine the crystal structure of the mineral phases, selected area electron diffraction (SAED) was carried out in TEM mode.

Analysis of approximately 50 particles of aged biochar extracted from soil samples at each depth was carried out to determine the range of particle types and their nominal composition. This gave a reliable indication of overall mineral content, which might be released when the biochar was applied to soil. The biochars were ground to pass through a 100-μm sieve before analysis. Surface functional groups and major mineral elements were measured using X-ray photoelectron spectroscopy (XPS) analysis (Thermo Scientific ESCALAB250Xi; Thermo Scientific, Waltham, USA) with a 500 μm diameter beam of monochromatic Al-$K\alpha$ radiation (photon energy = 1 486.6 eV) at a pass energy of 20 eV. The core level binding energies (BEs) were aligned with respect to the C1s BE of 285.0 eV. Fourier transform infrared spectroscopy (FTIR) analysis was carried out using the equipment and procedure as detailed in Joseph *et al.* (2010 and 2013). Raman spectroscopy was carried out using the equipment and procedure detailed in Chia *et al.* (2012). Since the particles contained a high content of mineral matter, 12 spectra were taken from near the mineral particles and from the C matrix. Two peak fitting was used to determine the ratio of D-band to G-band intensity (D/G ratio) and the particle size as per described in Chia *et al.* (2012). Analysis of variance (ANOVA) of the D/G ratios was carried out to determine if there was a significant difference between samples both near the mineral phase and on the C phase.

Solid-state nuclear magnetic resonance (NMR) spectroscopy

Solid-state ^{13}C cross polarization (CP) nuclear magnetic resonance (NMR) spectra of the fresh biochar were acquired (90° pulse of 3.2 μs, 195 W, relaxation delay 1 s) on a 200 Avance spectrometer (Bruker Corporation, Billerica, USA) equipped with a 4.7 Tesla wide bore superconducting magnet with a resonance frequency of 50.33 MHz for ^{13}C as described in Baldock and Smernik (2002). Chemical shifts were externally referenced to the methyl resonance of hexamethylbenzene (17.36 ppm) and a Lorentzian line broadening (50 Hz) applied.

The solid-state ^{13}C direct polarization magic angle spinning (DP-MAS) NMR experiments were carried out on the aged biochar on a Bruker AVANCE III 300 spectrometer (Bruker Corporation, Billerica, USA) employing a 7 Tesla super conducting magnet operating at frequencies of 300 and 75 MHz for the ^{1}H and ^{13}C, respectively. The biochar sample was finely ground, packed into a 4-mm zirconia rotor with Kel-F cap, and spun at 12 kHz before NMR analysis. The ratio of the protonated and non-protonated C in the char was determined according to the method of Brewer *et al.* (2009). [13]C-90° pulse length of 4 μs and 80 kHz ^{1}H SPINAL64 decoupling, along with a Hahn-echo before signal detection to eliminate baseline distortion, was used to acquire the spectra. A 68 AL64 decoupling, along with a Hahn-echo before signal detection was carried out to eliminate baseline distortion. The measurement time for the pair of ^{13}C DP-MAS experiments was 24 h.

Financial benefits of feeding biochar

Extensive interviews with the owner of the property and other farmers nearby were undertaken to determine the changes in costs in raising cows using biochar and molasses mixture, though it was recognized that this was not a comprehensive economic assessment of the value of feeding biochar to cattle, but provided a starting point for a more detailed study.

Statistical analysis

Analysis of ANOVA of the D/G ratios was carried out using Microsoft Office Excel to determine if there was a significant difference between biochar samples both near the mineral phase and on the C phase.

RESULTS

Bulk soil properties

The results of the soil tests carried out indicated that there was an increase in total organic carbon (TOC), pH (CaCl$_2$), Colwell P, Colwell K, EC and all of the exchangeable cations from the 2011 tests to the 2015 tests (Table I). Properties of the soil samples from the areas where biochar was extracted are given in Table II. Soil pH decreased only slightly from 6.2 to 5.8 from the surface (0–5 cm) to a depth of 40 cm, and soil EC decreased by approximately 50%. Colwell P and KCl-extractable NH$_4^+$-N in soil increased from 0–5 cm to 20–30 cm and then decreased at 30–40 cm. Total C, K and P, and exchangeable Ca, K, Mg, and Na in soil decreased by approximately 40%–60% at 20–30 cm.

Some physico-chemical properties of the soil samples from areas where biochar was extracted at three depths

Property[a]	0–5 cm	20–30 cm	30–40 cm
EC (dS m^{-1})	0.140	0.120	0.075
pH (CaCl$_2$)	6.2	6.1	5.8
Total N (g kg^{-1})	4.7	2.4	1.1
Total C (g kg^{-1})	60	36	20
Total P (g kg^{-1})	1.70	0.97	0.26
Total K (mg kg^{-1})	160	100	65
Colwell P	160	210	44
NH$_4^+$-N (mg kg^{-1})	20	28	25
NO$_3^-$-N (mg kg^{-1})	36.0	7.7	7.0
Al (g kg^{-1})	42	43	43
As (mg kg^{-1})	< 5.0	< 5.0	< 5.0
B (mg kg^{-1})	4.7	4.1	< 4.0
Ca (g kg^{-1})	3.80	2.00	0.99
Cd (mg kg^{-1})	< 0.3	< 0.3	< 0.3
Co (mg kg^{-1})	3.6	4.6	5.9
Cr (mg kg^{-1})	42	49	54
Cu (mg kg^{-1})	16.0	14.0	7.7
Fe (g kg^{-1})	42	53	60
K (mg kg^{-1})	160	100	65
Mg (mg kg^{-1})	560	370	200
Mn (mg kg^{-1})	130	130	98
Mo (mg kg^{-1})	1.6	1.4	1.3
Na (mg kg^{-1})	60	38	30
Ni (mg kg^{-1})	5.6	6.0	6.4
Pb (mg kg^{-1})	6.1	7.4	8.0
S (mg kg^{-1})	700	480	260
Se (mg kg^{-1})	< 4.0	< 4.0	< 4.0
Zn (mg kg^{-1})	22.0	15.0	3.7
Exchangeable cation			
Al (cmol(+) kg^{-1})	< 0.01	< 0.01	< 0.01
Ca (cmol(+) kg^{-1})	14.0	7.2	3.6
K (cmol(+) kg^{-1})	0.200	0.120	0.066
Mg (cmol(+) kg^{-1})	3.30	2.10	0.95
Na (cmol(+) kg^{-1})	0.120	0.075	0.054
CEC (cmol(+) kg^{-1})	18.0	9.4	4.7
Ca/Mg ratio	4.4	3.5	3.8

[a]EC = electrical conductivity; NH$_4^+$-N = KCl-extractable NH$_4^+$-N; NO$_3^-$-N = KCl-extractable NO$_3^-$-N; CEC = cation exchange capacity.

Properties of the fresh biochar

An image of the fresh biochar is given in Fig. 2. The structure was not typical of high-temperature woody biochar in that there was little evidence of very small pores (< 1 μm) within the larger 10–30 μm macro pores (Joseph *et al.*, 2010). The surface of these pores appeared to be covered with a layer of amorphous organic C. The proximate and ultimate analyses of fresh biochar are given in Table III. The total and fixed C and ash content were relatively high, which was a function of the high-temperature and the long residence time under which the biochar was produced. However, there was a significant concentration of organic compounds which could have resulted from condensa-

tion of volatiles during the production process. This would, in part, account for the low surface area of the biochar and the absence of visible small pores as shown in Fig. 2.

Proximate and ultimate analyses of the fresh biochar

Parameter	Proportion
	%
Proximate analysis	
Moisture	1.0
Ash	7.8
Volatile matter	16.2
Fixed C	75.0
Ultimate analysis	
Total C	82.0
H	2.0
N	0.4
Total S	0.03
O	15.57

The major minerals detected in the fresh biochar included silica, calcite and quartz. Important metals and non-metals (excluding Si) identified included 4 000 mg kg^{-1} Al, 2 500 mg kg^{-1} Fe, 3 000 mg kg^{-1} Ca, 1 200 mg kg^{-1} Na, 3 000 mg kg^{-1} S, 300 mg kg^{-1} K, 600 mg kg^{-1} Mg, 650 mg kg^{-1} P, and 650 mg kg^{-1} Zn. Dempster *et al.* (2012) measured total C as 851 g kg^{-1}, total N 6.9 g kg^{-1}, pH (1:5 H$_2$O) 8.41, EC 388 mS cm^{-1}, cation exchange capacity 9.5 mmol kg^{-1}. The proportion of aromatic C concentration was 69.1%, extractable C was 1 653 mg C kg^{-1}, and total pore area was approximately 8 m^2 g^{-1}. These values were low for high-temperature wood biochars and indicated that there had been condensation of volatiles on the pores of the biochar in the kiln. This was in agreement with observations from the SEM and NMR analyses, described below.

The NMR spectra (Fig. 3) showed a high concentration of aromatic (aryl) C (77%), but also a significant concentration of amorphous C with various oxygenated functional groups. This is typical of woody biochars in which there has been condensation of volatiles on the inner pores (Joseph *et al.*, 2010). Small amounts of alkyl, O-alkyl/methoxyl (< 6%), ketone (2%) and amide/carboxy (3%) groups (Table IV) were consistent with the results of the XPS analysis below. Again, this was consistent with high concentration of condensed organic compounds on the surface of the pores. It was probable that condensation occurred during cooling of the biochar in the kiln.

Table V shows the C and N functional groups found in the fresh biochar from the kiln prior to being fed to the cows. Although the biochar had been produced at
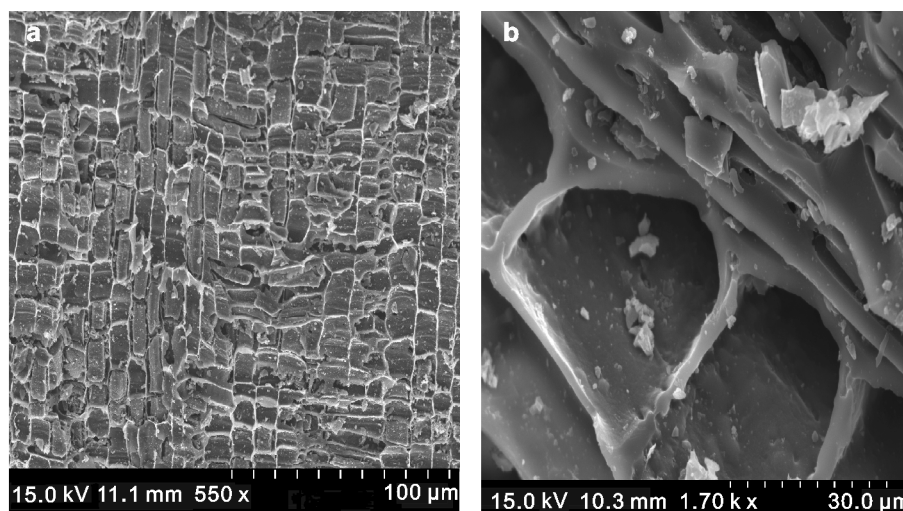
Fig. 2 Surface image of the jarrah wood biochar (a) and the image of pores (b) in the biochar using the scanning electron microscopy.
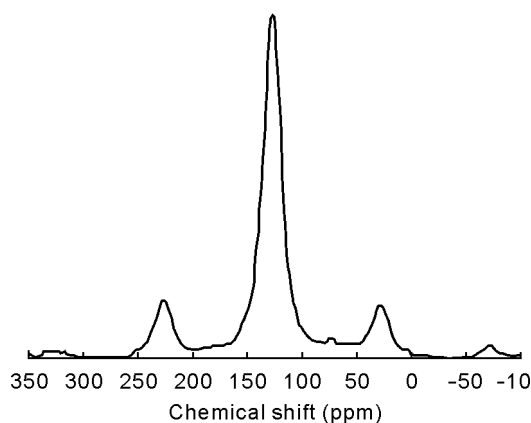

Fig. 3 Solid-state ^{13}C nuclear magnetic resonance (NMR) spectra of fresh jarrah wood biochar. Spinning side bands are found at 225 and 25 ppm.

TABLE IV

Integration of spectral regions and their chemical assignment from the solid-state ^{13}C nuclear magnetic resonance (NMR) spectra describing the C composition of the fresh jarrah wood biochar

Chemical shift	Assignment	Percentage of total C
ppm		%
0–45	Alkyl	< 1
45–60	N-alkyl/methoxyl	< 1
60–95	O-alkyl	4.5
95–110	Di-O-alkyl	4.5
110–145	Aryl	77
145–165	O-aryl	8
165–190	Amide/carboxyl	3
190–215	Ketone	2

high-temperatures, there was still a significant concentration of C–O, C=O and COOH groups on the surface of the fresh biochar, indicating that either some O had reacted with the surfaces either in the kiln or during the cooling process, or the surface had organic compounds rich in these functional groups. The concentrations of Al and Si are 12 and 30 g kg^{-1}, respectively, and are considered high for a wood biochar. Na, Fe and Mg form a significant component of the mineral matter on the surface of the biochar (Table VI).

The chemical compounds detected using GC-MS are presented in Table VII. There was a wide range of carboxylic acids and alkanes. Benzene, toluene, xylene, naphthalene and diisopropylnaphthalene isomers (2,6) were also detected in small quantities. Detailed quantification of these compounds was not carried out, although they were not considered a risk in high-temperature biochars (Kookana *et al.*, 2011). Further testing is needed to determine if any of these aromatic compounds has accumulated in the tissue of cow.

Properties of the biochar after digestion and incorporation into the soil

The biochar extracted from the soil samples taken across the transect to a depth of 10 cm had a total C content of 640 g kg^{-1}, total N of 14 g kg^{-1}, total P of 1.1 g kg^{-1}, total K of 0.62 g kg^{-1}, Mg of 0.72 g kg^{-1}, Ca of 5.3 g kg^{-1}, S of 1.5 g kg^{-1}, pH (CaCl$_2$) of 6.71, EC of 0.163 mS cm^{-1}, Colwell P of 700 mg kg^{-1}. Visually, the biochar had a coating of clay and other mineral matter was reflected in a Fe content of 57 g kg^{-1} and Al of 42 g kg^{-1}.

Scanning electron microscopy images of the biochar from fresh dung and from soil samples at 0–5, 20–30 and 30–40 cm are given in Fig. 4a, c, e and g, respectively. It was observed that the biochar extracted from the fresh dung and from soil sample at 0–5 cm (Figs. 4a and 4c) had an outer coating of organo-mineral com-

TABLE V

Regional scan of C and N functional groups in various biochars using the X-ray photoelectron spectroscopy

Peak	Function group	Biochar[a]				
		Fresh biochar	D0	D1	D2	D3
		atom%				
C1s A	C–C/C–H/C=C	64.20	52.29	59.17	50.25	66.35
C1s B	C–O	11.43	16.23	15.31	13.96	11.44
C1s C	C=O	3.61	6.84	5.31	4.41	2.31
C1s D	COOH	2.21	2.75	3.43	4.04	3.61
C1s E	Carbonate	1.55	nd[b]	nd	nd	nd
N1s A	Amino acid N/N–C=O	0.48	3.76	1.77	0.86	0.65
N1s B	NH_4/NH_2	0	0.70	0.14	0.10	nd
N1s C	Pyridine/N–O	0	0.50	0.09	nd	nd

[a] D0 = biochar extracted from freshly deposited cow dung; D1, D2 and D3 = biochar extracted from soil samples at 0–5, 20–30 and 30–40 cm, respectively.
[b] Not detectable.

TABLE VI

Regional scan of elements in various biochars using the X-ray photoelectron spectroscopy

Name	Biochar[a]				
	Fresh biochar	D0	D1	D2	D3
	atom %				
C1s	78.85	76.63	81.63	68.52	80.05
O1s	15.41	16.90	14.11	23.63	15.36
N1s	0.75	4.54	2.04	1.08	0.70
Na1s	0.35	0.33	0.25	0.21	1.10
Mg1s	0.20	0.62	0.34	0.5	0.22
P2p	nd[b]	nd	0.19	nd	nd
Ca2p	nd	nd	0.40	nd	nd
Fe2p	0.19	0.63	0.11	0.15	0.27
Cl2p	0.08	0.13	0.21	0.23	1.06
Si2p	2.96	0.02	1.02	2.30	1.23
Al2p	1.21	0.20	0.29	3.38	nd

[a] D0 = biochar extracted from freshly deposited cow dung; D1, D2 and D3 = biochar extracted from soil samples at 0–5, 20–30 and 30–40 cm, respectively.
[b] Not detectable.

TABLE VII

Some labile organic compounds extracted from the jarrah wood biochar detected by the gas chromatography-mass spectrometry

Species	Compounds
Carboxylic acid	Dodecanoic acid, tetradecanoic acid, hexadecanoic acid, heptadecanoic acid, cis-9-octadecenoic acid, trans-9-octadecenoic acid, octadecanoic acid, eicosanoic acid, docosenoic acid (isomer), docosanoic acid, tetracosanoic acid
Alkanes	Dodecane, tridecane, tetradecane, pentadecane, hexadecane, heptadecane, octadecane, nonadecane, eicosane
Aromatic hydrocarbon	Toluene, xylenes, 1,2,3-trimethyl benzene, naphthalene, diisopropylnaphthalene isomers (2,6)
Other	4-hydroxy-3,5-dimethoxy-denzaldehyde, dibutyl phthalate

plex which had a high concentration of nutrients (P, K, N, Mg, Ca) and minerals rich in Al, Si and Fe. At lower depths there was a much lower concentration of nutrients and a visible coating rich in Al, Si and Fe (probably clay, SiO_2, Fe oxides, alumina). These observations were similar to those reported by Joseph *et al.* (2010) and Lin *et al.* (2012b).

The TEM and STEM images of minerals on the surface of the biochar extracted from soil sample at 0–5 cm are shown in Fig. 5a and d, respectively. The biochar surface had mineral phase particles of 2–10 nm in diameter and a range of irregular pores were present with sizes ranging from 2 to 100 nm. The EDS (data not shown), SAED (Fig. 5b) and EELS analyses (Fig.
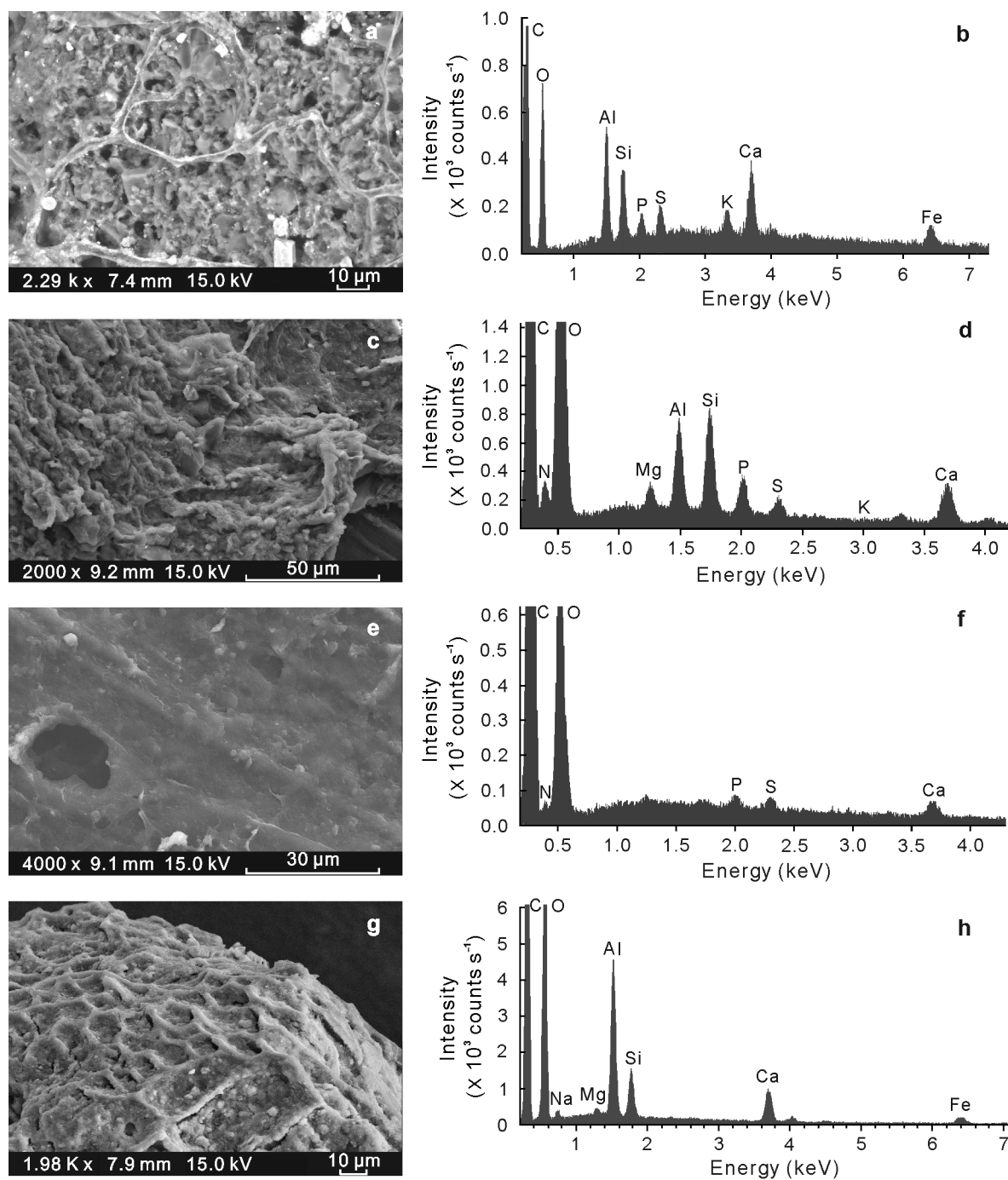
Fig. 4 Scanning electron microscopy images of the biochar extracted from the freshly deposited cow dung (a) and from soil samples at 0–5 cm (c), 20–30 cm (e) and 30–40 cm (g); and the corresponding energy dispersive X-ray spectrometer spectra (b, d, f and h) showing the major elements on the surface of the biochar.

5c) indicated that the minerals on the surface of the biochar were mainly SiO_2, Al_2O_3, and Fe_3O_4. Within the C lattice and the minerals there was a low concentration of P, Cl, K, Ca, S, Cl. Similar structures were seen in samples taken from the 20–30 and 30–40 cm layers, although there was a higher concentration of Al/Si/Fe nano-particles in the latter sample (data not shown).

Fig. 6 and Table VIII show the results of the quantitative analysis of the ^{13}C spectra in the biochar extracted from the top 10 cm of soil along a transect. The biochar still had a high concentration of nonprotonated C (57% of the total C in the extracted biochar), indicating a high degree of aromatic condensation. Total aromatic C (excluding the phenolic compounds) in this aged biochar was measured at 69%
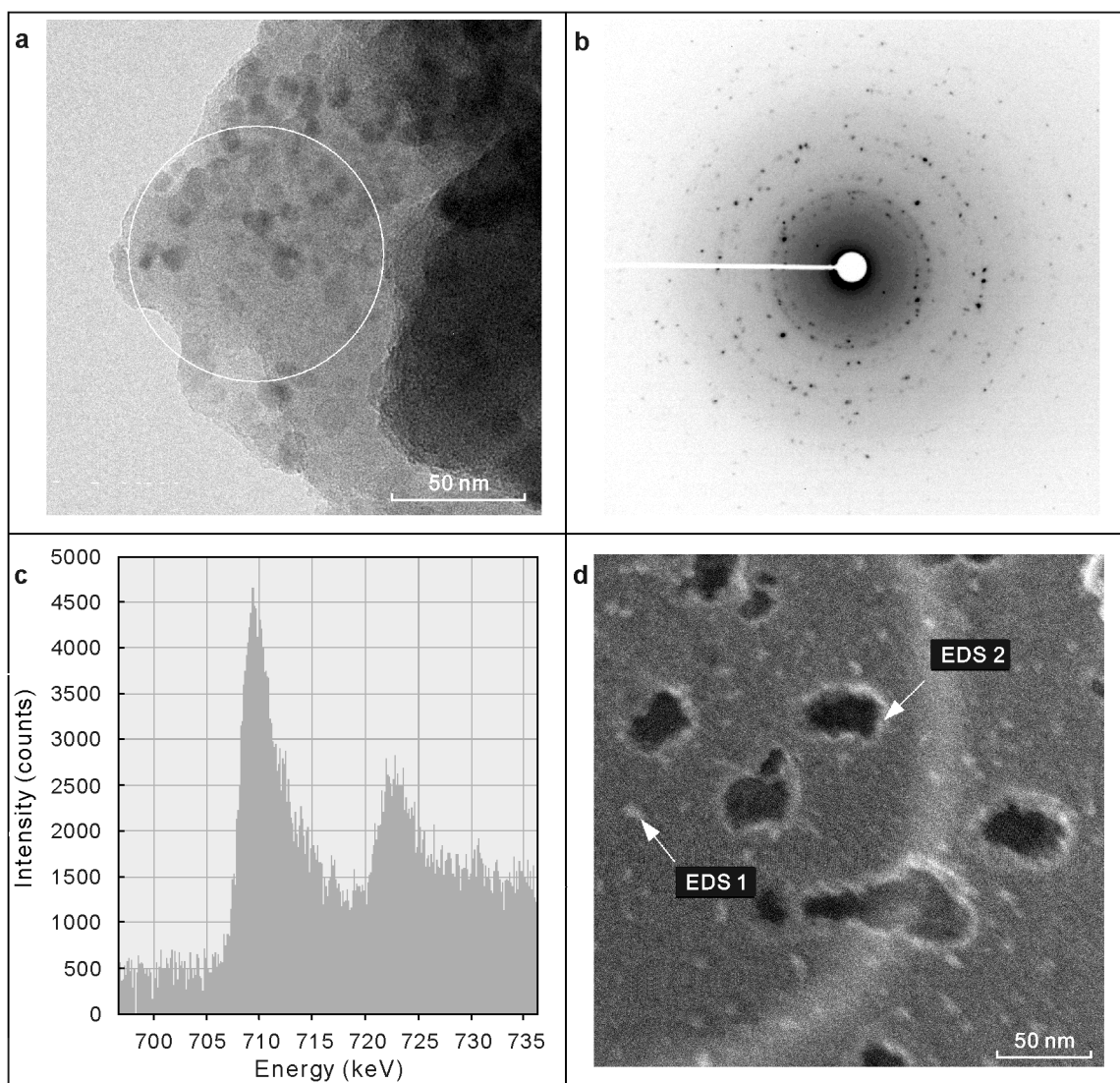
Fig. 5 (a) Transmission electron microscopy (TEM) image of the minerals on the surface of the biochar extracted from soil sample at 0–5 cm; (b) selected area electron diffraction (SAED) pattern from the circle area in (a); (c) Fe electron energy loss spectrometer (EELS) spectra from the circle area in (a); (d) scanning transmission electron microscopy (STEM) image highlighting the presence of minerals (bright, EDS1) and pores (dark, EDS2) in the biochar.
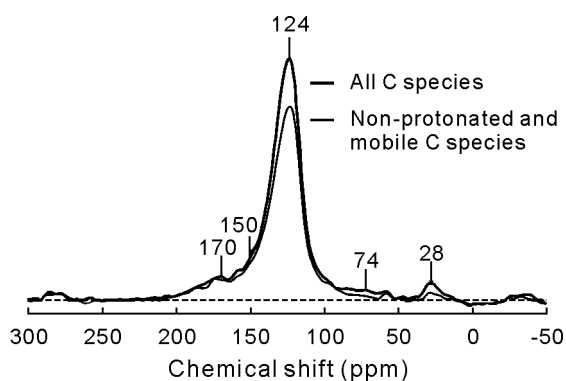

Fig. 6 Quantitative ^{13}C direct polarization magic angle spinning (DP/MAS) nuclear magnetic resonance (NMR) spectra of the biochar extracted from the top 10 cm of soil along a transect. The spinning side bands are found at approximately 295 and −35 ppm. The dotted line is a base line.

which was similar to that measured for the fresh biochar. Additionally, there was a high concentration of phenolic (9%), ketonic (5%) and carboxylic (6%) groups. This would indicate that the adsorption of organic matter with a high concentration of C functional groups had occurred, along with oxidation of the C. This has been recorded in biochars extracted from similar soil (Joseph *et al.*, 2010).

The XPS results indicated that, as a function of depth, there were differences in the surface C and N functional groups and in the type and concentration of minerals present within the extracted aged biochars (Tables V and VI). The biochar extracted from the dung had a higher organic C concentration, being rich in alcoholic, phenolic, hydroxyl, and/or other groups,

TABLE VIII

Integration of spectral regions and their chemical assignment from the ^{13}C nuclear magnetic resonance (NMR) spectra describing the C composition of the biochar extracted from the top 10 cm of soil along a transect

Chemical shift	Assignment[a]	Percentage of total C
ppm		%
201–183	C=O	4
183–165	COO	5
165–145	C_{ar}-$O_{75}H_{0.5}$	9
145–90	$C_{ar-nonprot}$	57
145–90	C_{ar-H}	12
90–50	$HCO_{0.75}H_{0.5}$	9
50–25	$CH_{1.5}$	3
25–6	CH_3	2

[a]C_{ar}-$O_{75}H_{0.5}$ = phenolic C; $C_{ar-nonprot}$ = non-protonated aromatic C; C_{ar-H} = protonated aromatic C.

C=O and COOH groups compared with the fresh biochar taken directly from the kiln. The concentration of COOH groups increased as the biochar aged with a maximum concentration at the depth of 20–30 cm. This was consistent with the findings of other authors (Cheng *et al.*, 2006). Three distinct classes of N functional groups (NH_4/NH_2, amino acid/N–C=O, pyridine/N–O) were detected in the biochar after passing through the animal gut and being buried to a depth of 30 cm. The amino acid/N–C=O functional groups were at higher concentrations compared with the fresh biochar.

Ca and P were detected on the surface of biochar particles at a depth of 0–5 cm but not with the other samples. This was consistent with the results of the soil/biochar analysis given in Tables II and III and the EDS spectrum given in Fig. 4. The O and Al/Si concentrations in the biochar reached a maximum at a depth of 20–30 cm, indicating that maximum reactivity occurred with the Fe/Al/Si-bearing minerals as the pH and the O concentration in the soils decreased and the biochar had been incorporated for a significant period. These data were consistent with the results reported by Joseph *et al.* (2010) and Lin *et al.* (2012b) where the mineral formation on the surface of the biochar reached a maximum following 1–2 years of incorporation into the soil. They have postulated that it is the formation of these highly porous, redox-active organo-mineral complexes on the surface of the biochar which drives the increased availability of nutrients and changes in other soil properties over a long period of time.

The Raman spectra were modeled using two Gaussian functions located at positions characteristic of the D- and G-bands. These measure the degree of structure of trigonal sp2 hybridised C in aromatic sheet struc-

tures formed in biochar. Increased D/G ratio indicated more defects in the flat layers of sp2 hybridised C, which maked up the graphene-like phase in biochar. The average D/G ratio for the fresh biochar was found to be 2.22 with a range of 1.83 to 2.38 (D-band 1 380 cm^{-1}, G-band 1 589 cm^{-1}) compared to 2.0 for the biochar extracted from the fresh dung. The D/G ratio of the biochar extracted from the soil sample varied from an average of 1.96 to 2.29 with the ANOVA result indicating no significant differences between these values ($P = 0.1197$, Table IX). These results indicated that there was very little or no change in the nature of the C lattice.

TABLE IX

Detailed analysis of variance (ANOVA) of the Raman spectral data of various biochars

Source of variation	Sum of squares	df[a]	Mean square	F-value	P-value
Between groups	0.5930	4	0.1482	1.9456	0.1197
Within groups	3.3527	44	0.0762		
Total	3.9458	48			

[a]Degree of freedom.

Similarities between FTIR spectra enabled the biochars to divided into two groups: D0 (from fresh dung), D1 (0–5 cm) and D2 (20–30 cm) biochars; D3 biochar (30–40 cm) and the fresh biochar (Fig. 7). The biochar from fresh dung had more intense peaks for aliphatic O–H and O–H stretching in alcohols and phenols as well as a C–H deformation indicating lignins compared with that from 0–5 and 20–30 cm. There was only a very low intensity of these vibrational modes in the biochar from 30–40 cm and none in the fresh biochar. The presence of aromatic C=C was seen in all
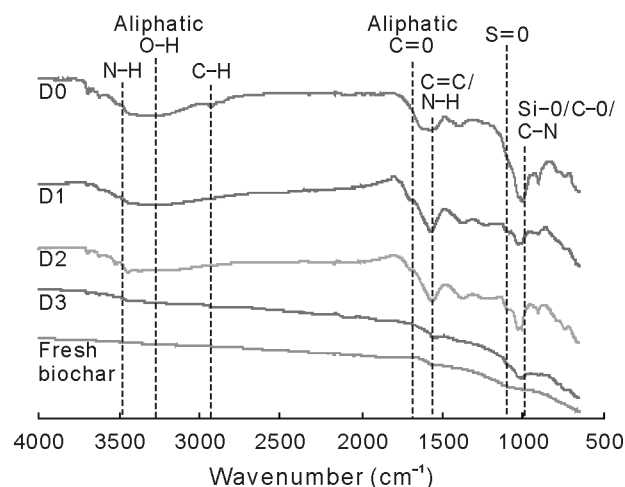

Fig. 7 Fourier transform infrared spectroscopy spectra of fresh jarrah wood biochar and the biochar extracted from freshly deposited cow dung (D0) and from soil samples at three depths of 0–5 (D1), 20–30 (D2), and 30–40 cm (D3).

the four biochars between $1\,690$ and $1\,610$ cm^{-1} with the highest intensities in D0–D2 biochars. It should be noted that the N–H bend peak also occurred at these wavenumbers. The peaks at approximately $1\,775$–$1\,710$ cm^{-1} originated from C=O functional groups and were only significant for D0–D2. Except for the fresh biochar, the D0–D3 biochars had a relatively high intensity at $1\,101$–$1\,160$ cm^{-1} which represented C–O stretching in acids, phenols, ethers or esters and at $1\,035$–990 cm^{-1} in Si–O–Si. The D0–D2 biochars had a relatively high intensity of peaks associated with amines ($3\,500$–$3\,300$, $1\,640$–$1\,500$ and $1\,025$–$1\,200$ cm^{-1}, respectively).

An initial assessment of financial benefits of feeding biochar

The following is an initial financial assessment of the relative yearly costs of raising 60 cows involving the use of application of chemical fertilisers to pastures, hay supplements and chemical drenching. Costings were carried out for 3 different options for provision of hay. In the first conventional practice (CP1) the farmer buys in hay; the second one (CP2) the farmer grows hay and pays a contractor to harvest the hay, and in the third one (CP3) the farmer grows and harvests the hay himself. These conventional methods were compared with the practice of feeding biochar and molasses to cows (biochar practice).

Conventional practice sees calving in January–February with calves being sold in November–December. In biochar practice calving occurs in July–August. Half of the calves are sold in the following June and another half in December. This practice was developed to adapt to the changing weather patterns. The farmer made the following observation: "It is now much warmer all year, the winters are wet but not nearly as wet (as in previous years) and the summers are much hotter and very dry. Summer is now the stress season for cattle. Pasture growth is excellent through winter, more sun, warmer days and nights, and not so waterlogged. The perennial grasses are dying out on the hills as the summers are too hot and dry for so long months. Thus, I have changed mating to ensure that calving occurs when at a time of year that makes the peak nutritional demand on the cow coincident with maximum feed availability. I believe that selling two times a year to two markets is a hedge against market fluctuations actually"

This change in strategy resulted in slightly lower income but more certainty of long-term viability of the farm. The following assumptions have been considered to develop Table X: i) number of cow/calf breeding units are the same per area (60 cows per 40 ha), ii) pasture is the same mix of perennial and annual grasses, iii) topography is the same proportion of summer dry hills and summer moist flats, iv) soil types are the same mix of heavy Vertisol clay flats, medium red to brown Chromosols, lighter red to brown Kandosols and some lateritic gravel, v) paddock sizes and water requirements are the same, vi) rotational grazing is similarly practiced, vii) animal breed and ages are the same, viii) value of all cow herds is equal, ix) for CP, 60 calves are sold at \$900 with total value \$54\,000, and x) for biochar practice, 30 calves are sold at \$750 and 30 calves at \$900 with total value \$49\,500. This simple analysis indicates that the profitability may be higher for biochar practice compared with CP.

TABLE X

Cost of feeding 60 cows year^{-1} using conventional practice (CP) compared with biochar practice.

Item	CP1	CP2	CP3	Biochar practice
Fertiliser	\$5\,210	\$5\,210	\$6\,630	0
Drench	\$600	\$600	\$600	0
Insect spray	\$500	\$500	\$500	0
Hay	\$15\,600	\$13\,200	\$7\,000	0
Maintenance/depreciation	0	0	\$3\,000	0
Biochar/molasses	0	0	0	\$1\,000
Total cost	\$21\,910	\$19\,510	\$17\,730	\$1\,000
Income	\$54\,000	\$54\,000	\$54\,000	\$49\,500
Income $-$ cost	\$32\,090	\$34\,490	\$36\,270	\$48\,500

DISCUSSION

Using activated C, charcoal, humic acids and wood vinegar as both a feed supplement and for medicinal purposes has proven effective in a number of studies (Neuvonen and Olkkola, 1988; Van *et al.*, 2006, Gerlach *et al.*, 2014). Jarrah wood biochar, before it enters into the stomach, has both a relatively high concentration of oxygenated functional groups and a small concentration of organic molecules. These have characteristics of humic acids, biopolymers, low molecular weight acids and neutrals (Lin *et al.*, 2012a) and a small amount of benzene, toluene, xylene and naphthalene. Jarrah wood biochar had a range of organic molecules similar to some of those found in wood vinegar. Its pH is similar to the saliva that is in the mouth of the cow and thus may have the same buffering capability (Church, 1987).

Once the biochar enters to the stomach it is involved in both biotic and abiotic chemical reactions in both acidic and alkaline environments. The research of Lin *et al.* (2012a) indicates that the concentration of O and N functional groups will change and the biochar

will probably release a much larger quantity of labile organic molecules, some of which have characteristics of humic acids and others that are low molecular acids and neutrals. The release of these molecules can act as a biocide (Watarai *et al.*, 2008). There will also be a release of minerals from the biochar which may be beneficial for the growth of the cow. Once these fermentation and acid base reactions have taken place (as indicated by the XPS results of the biochar extracted from the fresh dung) the reactivity of the surfaces of the biochar will probably increase (Joseph *et al.*, 2013). These functional groups could play an active role in adsorbing toxins and possibly in the transformation of organic matter to carbohydrates, sugars and proteins in the rumen of the cow, as has been alluded to in the literatures (Van *et al.*, 2006; Villalba *et al.*, 2002; Watarai *et al.*, 2008). The activated biochar could also adsorb signaling compounds as noted by Masiello *et al.* (2013) which exist in the rumen and change gene expression and microbial population, although the evidence for this is not conclusive (Ermolaeva *et al.*, 1997, 1999, 2004). The complex role of biochar in disease suppression in cows needs much more in-depth study.

The chemical and spectral analysis and imaging of the biochar that were extracted from the fresh dung clearly showed that the biochar adsorbed a range of nutrients in the rumen. These nutrients (especially P and N) were retained in the biochar when incorporated into soils to a depth of at least 10 cm and are plant available. Given the fact that the farmer does not need to apply fertilizer, the biochar is probably a major factor in nutrient availability. The high N concentration of the biochar that has been incorporated in the dung was consistent with the concentrations of N found in biochar extracted from compost (Clough *et al.*, 2013). The N decreased once the biochar was incorporated into the soil and could indicate utilization by the pasture plants and soil microbes. The measurement of the NH_4/NH_2 and pyridine/N–O groups indicates that N compounds have been adsorbed into the C lattice or are part of organo-mineral complexes that have formed as biochar ages in the soil (Joseph *et al.*, 2010 and 2013)

Nanoscale examination of the biochars in the top 20 cm of soil indicated that there was a relatively high concentration of Fe oxide nano-particles. The SAED pattern indicated that these nano-particles are a mixture of magnetite and hematite. Fe nano-particles can play an important role in many biotic and abiotic processes especially in environments where Eh can change. Amonette *et al.* (2006) noted that tyrosinase, a phenol oxidase enzyme that assists in the breakdown of

organic matter, has been suggested to be promoted in the presence of highly microporous charcoal and nano-particulate Fe oxides. Li *et al.* (2012) noted that Fe oxide particles can be involved in a complex series of redox reactions involving the breakdown of humic substances and the conversion of N in organic matter to either NO_3^- or NH_4^+ ions and the breakdown of P containing organic compounds to available P. This could be a factor in the increase in available P and N in the soil. Significantly more research is required to determine if the Fe nano-particles are catalyzing these types of reactions.

It would appear that there has been very little change in the recalcitrant C structure of the biochar as a result of digestion in the rumen and after interaction with dung beetles and movement through the soil profile. This would be expected as the high pyrolysis temperature and the long residence time in the kiln has produced a high concentration of condensed aromatic rings which are recalcitrant (Singh *et al.*, 2012). Following incorporation into the soil, at lower depths biochar has reacted with soil organic and mineral matter to form a coating of organic mineral complexes. This may increase the stability and the lifetime of the C. Further detailed investigation of the stability of these particles need to be undertaken using incubation trials as per the techniques described by Singh *et al.* (2012).

CONCLUSIONS

Feeding cows a mixture of high-temperature wood biochar and molasses has had the potential to reduce costs for the farmer, to improve soil properties, and to improve pasture health. Dung beetles moved the dung and biochar through the soil horizon to increase stable C and to enhance soil fertility. The C lattice of biochar appeared to undergo minimal changes as it passed through the gut of the animal. The biochar-dung composite had a high N concentration and there was an increase in C–O and C–OOH functional groups. Once in the soil the biochar started to age through interaction with soil organic and mineral matter. Available P and N concentrations of the soil around the biochar increased due to a series of complex reactions. These changes could occur over a range of depths as biochar was taken through the soil profile quickly by dung beetles.

Aside from the scientific merits of this approach, a basic financial assessment suggested that there may have economic benefits as well. This study provided very positive and initial evidence that biochar practice

could be commercialized very quickly. More detailed research needs to be undertaken to evaluate a range of soil types, using different biochar types, biochar/molasses ratios, and dosage rates and dung beetles species. There is a need to analyse accurately costs and benefits to the farmer and also the feasibility of this method for long-term sequestration of C into soils. Further tests need to be carried out to determine if there are any residual toxins, such as polycyclic aromatic hydrocarbons or dioxins, which have accumulated in the meat of the cattle.

ACKNOWLEDGEMENTS

REFERENCES

Amonette J, Kim J, Russell C, Hendricks M, Bashore C, Rieck B. 2006. Soil charcoal—a potential humification catalyst. ASA-CSSA-SSSA International Annual Meetings, Indianapolis, USA. November 12–16, 2006.

Baldock J A, Smernik R J. 2002. Chemical composition and bioavailability of thermally altered *Pinus resinosa* (red pine) wood. *Org Geochem.* **33**: 1093–1109.

Blackwell P, Riethmuller G, Collins M. 2009. Biochar application to soil. *In* Lehmann J, Joseph S (eds.) Biochar for Environmental Management: Science and Technology. Earthscan, London. pp. 207–226.

Brewer C E, Schmidt-Rohr K, Satrio J A, Brown R C. 2009. Characterization of biochar from fast pyrolysis and gasification systems. *Environ Prog Sust Energ.* **28**: 386–396.

Calvelo Pereira R, Muetzel S, Camps Arbestain M, Bishop P, Hina K, Hedley M. 2014. Assessment of the influence of biochar on rumen and silage fermentation: A laboratory-scale experiment. *Anim Feed Sci Tech.* **196**: 22–31.

Cheng C H, Lehmann J, Thies J E, Burton S D, Engelhard M H. 2006. Oxidation of black carbon by biotic and abiotic processes. *Org Geochem.* **37**: 1477–1488.

Chia C H, Marjo C E, Gong B, Joseph S D, Munroe P, Rich A M. 2012. Imaging of mineral-enriched biochar by FTIR, Raman and SEM-EDX. *Vib Spectrosc.* **62**: 248–257.

Chia C H, Singh B P, Joseph S, Graber E R, Munroe P. 2014. Characterization of an enriched biochar. *J Anal Appl Pyrol.* **108**: 26–34.

Church D C. 1987. The Ruminant Animal: Digestive Physiology and Nutrition. Prentice Hall, Englewood Cliffs.

Clough T J, Condron L M, Kammann C, Müller C. 2013. A review of biochar and soil nitrogen dynamics. *Agronomy.* **3**: 275–293.

Dairy Australia. 2015. Hay and grain market report. Available online at http://www.dairyaustralia.com.au/Pastures-and-Feeding/Supplements-and-nutrition/Supplementary-feeds-2/National–Hay-Grain-Market-Report/South-West-WA.aspx (verified on July 22, 2015)

Dempster D N, Jones D L, Murphy D V. 2012. Clay and biochar amendments decreased inorganic but not dissolved organic nitrogen leaching in soil. *Aust J Soil Res.* **50**: 216–221.

Doube B, Dalton G, Ford R. 2003. The potential of dung beetles to improve the quality of catchment water in Australia. The First National Conference on Integrated Catchment Management, held at the University of Western Sydney, Parramatta. November 26–27, 2003.

Downie A E, Van Zwieten L, Smernik R J, Morris S, Munroe P R. 2011. *Terra Preta Australis*: reassessing the carbon storage capacity of temperate soils. *Agr Ecosyst Environ.* **140**: 137–147.

Ermolaeva S, Belyi Y, Tartakovskii I. 1999. Characteristics of induction of virulence factor expression by activated charcoal in *Listeria monocytogenes. FEMS Microbiol Lett.* **174**: 137–141.

Ermolaeva S, Novella S, Vega Y, Ripio M T, Scortti M, Vázquez-Boland J A. 2004. Negative control of *Listeria monocytogenes* virulence genes by a diffusible autorepressor. *Mol Microbiol.* **52**: 601–611.

Ermolaeva S, Varfolomeeva N, Belyi Y, Tartakovskii I. 1997. Isolation and characterization of a *Listeria monocytogenes* mutant strain hyperproducing virulence factors. *FEMS Microbiol Lett.* **150**: 189–195.

Fincher G T. 1981. The potential value of dung beetles in pasture ecosystems. *J Georgia Entomol So.* 16: 316–333.

Gerlach H, Gerlach A, Schrödl W, Schottdorf B, Haufe S, Helm H, Shehata A, Krüger M. 2014. Oral application of charcoal and humic acids to dairy cows influences *Clostridium botulinum* blood serum antibody level and glyphosate excretion in urine. *J Clin Toxicol.* **4**: 186, doi: 10.4172/2161-0495. 1000186.

Hale S, Hanley K, Lehmann J, Zimmerman A R, Cornelissen G. 2011. Effects of chemical, biological, and physical aging as well as soil addition on the sorption of pyrene to activated carbon and biochar. *Environ Sci Technol.* **45**: 10445–10453.

Haynes R J, Naidu R. 1998. Influence of lime, fertilizer and manure applications to soil organic matter content and soil physical conditions: A review. *Nutr Cycl Agroecosys.* 51: 123–137.

Joseph S D, Camps-Arbestain M, Lin Y, Munroe P, Chia C H, Hook J, van Zwieten L, Kimber S, Cowie A, Singh B P, Lehmann J, Foidl N, Smernik R J, Amonette J E. 2010. An investigation into the reactions of biochar in soil. *Aust J Soil Res.* **48**: 501–515.

Joseph S D, Graber E R, Chia C, Munroe P, Donne S, Thomas T, Nielsen S, Marjo C, Rutlidge H, Pan G X, Li L, Taylor P, Rawal A, Hook J. 2013. Shifting paradigms: Development of high-efficiency biochar fertilizers based on nano-structures and soluble components. *Carbon Manage.* **4**: 323–343.

Kookana R S, Sarmah A K, Van Zwieten L, Krull E, Singh B. 2011. Biochar application to soil: agronomic and environmental benefits and unintended consequences. *Adv Agron.* **112**: 103–144.

Li Y C, Yu S, Strong J, Wang H L. 2012. Are the biogeochemical cycles of carbon, nitrogen, sulfur, and phosphorus driven by the "Fe^{III}-Fe^{II} redox wheel" in dynamic redox environments? *J Soils Sediment.* **12**: 683–693.

Lin Y, Munroe P, Joseph S, Henderson R, Ziolkowski A. 2012a. Water extractable organic carbon in untreated and chemical treated biochars. *Chemosphere.* **87**: 151–157.

Lin Y, Munroe P, Joseph S, Kimber S, Van Zwieten L. 2012b. Nanoscale organo-mineral reactions of biochars in a ferrosol: an investigation using microscopy. *Plant Soil.* **357**: 369–380.

Masiello C A, Chen Y, Gao X, Liu S, Cheng H Y, Bennett M R, Rudgers J A, Wagner D S, Zygourakis K, Silberg J J. 2013. Biochar and microbial signaling: production conditions determine effects on microbial communication. *Environ Sci Technol.* **47**: 11496–11503.

McHenry M P. 2010. Carbon-based stock feed additives: A research methodology that explores ecologically delivered C biosequestration, alongside live weights, feed use efficiency, soil nutrient retention, and perennial fodder plantations. *J Sci Food Agr.* **90**: 183–187.

Neuvonen P J, Olkkola K T. 1988. Oral activated charcoal in the treatment of intoxications. Role of single and repeated doses. *Med Toxicol Adv Drug.* **3**: 33–58.

Singh B P, Cowie A L, Smernik R J. 2012. Biochar carbon stability in a clayey soil as a function of feedstock and pyrolysis temperature. *Environ Sci Technol.* **46**: 11770–11778.

Van D T T, Mui N T, Ledin I. 2006. Effect of method of processing foliage of *Acacia mangium* and inclusion of bamboo charcoal in the diet on performance of growing goats. *Anim Feed Sci Tech.* **130**: 242–256.

Van Zwieten L, Kimber S, Morris S, Chan K Y, Downie A, Rust J, Joseph S, Cowie A. 2010. Effects of biochar from slow pyrolysis of papermill waste on agronomic performance and soil fertility. *Plant Soil.* **327**: 235–246.

Villalba J J, Provenza F D, Banner R E. 2002. Influence of macronutrients and activated charcoal on intake of sagebrush by sheep and goats. *J Anim Sci.* **80**: 2099–2109.

Watarai S, Tana, Koiwa M, 2008. Feeding activated charcoal from bark containing wood vinegar liquid (Nekka-Rich) is effective as treatment for cryptosporidiosis in calves. *J Dairy Sci.* **91**: 1458–1463.